



Published in final edited form as:

Heart Rhythm. 2009 July ; 6(7): 1009–1017. doi:10.1016/j.hrthm.2009.03.029.

Mechanisms of Stretch Induced Atrial Fibrillation in the Presence and the Absence of Adreno-Cholinergic Stimulation: Interplay between Rotors and Focal Discharges

Masatoshi Yamazaki, MD, PhD^{1,3}, Luis M. Vaquero, PhD², Luqia Hou, MS¹, Katherine Campbell, MS¹, Sharon Zlochiver, PhD¹, Matthew Klos, BSc¹, Sergey Mironov, PhD¹, Omer Berenfeld, PhD¹, Haruo Honjo, MD, PhD³, Itsuo Kodama, MD, PhD³, José Jalife, MD, FHR¹, and Jérôme Kalifa, MD, PhD¹

¹ Center for Arrhythmia Research, University of Michigan, Ann Arbor, MI

² Telefonica I+D, Madrid, Spain

³Research Institute of Environmental Medicine, Nagoya University, Nagoya, Japan

Abstract

BACKGROUND—Both atrial stretch and combined adreno-cholinergic stimulation (ACS) have been shown to favor initiation and maintenance of atrial fibrillation (AF). Their respective contribution to the electrophysiological mechanism remains, however, incompletely understood.

OBJECTIVE—We endeavored to determine the mechanism of maintenance of stretch-related AF (SRAF) in the presence and absence of ACS, and to assess how focal discharges interact with rotors to modify the level of complexity in the activation patterns to perpetuate AF.

METHODS—Video imaging of AF dynamics was carried out using a SRAF model in isolated sheep hearts (n=24). Pharmacological approaches were used to (i) mimic ACS with acetylcholine (1 μ M) plus isoproterenol (0.03 μ M); and (ii) abolish triggered activity, in response to sarcoplasmic reticulum calcium release, with caffeine (5 mM, CA) or ryanodine (10-40 μ M, RYA).

RESULTS—In the absence of ACS, upon perfusion of CA or RYA, focal discharges were abolished and SRAF terminated in most of the cases (10/13 experiments). In the presence of ACS, multiple drifting rotors as well as a large number of focal discharges were identified and only 1/11 AF episodes terminated.

CONCLUSIONS—In the absence of ACS, SRAF is maintained by high-frequency focal discharges that generate fibrillatory conduction and wavebreaks. In the presence of ACS, SRAF dynamics is characterized by multiple high frequency rotors that are rendered unstable by spatially distributed focal discharges.

Address correspondence to: Dr. Jérôme Kalifa Center for Arrhythmia Research 5025 Venture Drive, Ann Arbor, MI 48108 Fax: 1-734-998-7784 E-mail: kalifaj@med.umich.edu .

Disclosures: None

Publisher's Disclaimer: This is a PDF file of an unedited manuscript that has been accepted for publication. As a service to our customers we are providing this early version of the manuscript. The manuscript will undergo copyediting, typesetting, and review of the resulting proof before it is published in its final citable form. Please note that during the production process errors may be discovered which could affect the content, and all legal disclaimers that apply to the journal pertain.

Keywords

Atrial fibrillation; Adreno-cholinergic stimulation; Ryanodine; Optical mapping

Introduction

Atrial dilatation and stretch have been widely recognized as major pathophysiological factors in the initiation and maintenance of atrial fibrillation (AF).^{1,2} Previously, we demonstrated that atrial stretch, induced by increasing levels of intra-atrial pressure during AF, increases the frequency and spatio-temporal organization of electrical waves emanating from the pulmonary veins area.³ It has also been known for many years that extrinsic cardiac autonomic input to the heart is important in AF initiation and maintenance.^{4,5} Many studies in patients and in animals have demonstrated that both vagal and sympathetic input have the propensity to initiate AF.^{4,6} For instance, it was shown that AF could be successfully terminated after radio-frequency delivery to atrial areas containing cardiac ganglionated plexi, which have been suggested to function as modulators of autonomic input to the heart.⁷ Further, recent studies have suggested that through its well-known actions of opening acetylcholine activated potassium (K_{ACh}) channels and increasing intracellular calcium, combined adrenergic and cholinergic stimulation (ACS) leads to both action potential duration (APD) shortening and late phase-3 early after-depolarizations (EADs)⁸ or delayed after-depolarizations (DADs);⁵ the resulting focal discharges (FDs), were expected to promote AF initiation.

The above studies notwithstanding, the precise mechanisms of AF *maintenance* in the presence of atrial stretch with or without autonomic stimulation remain incompletely explored. Here, we utilized a stretch-related AF (SRAF) model in isolated sheep hearts, optical mapping techniques and a pharmacological approach to investigate AF dynamics associated with atrial stretch alone, or in the continuous presence of ACS, before and after FDs were abolished pharmacologically. Specifically we examined the respective roles of reentry and FDs in the setting of stretch and ACS. We hypothesized that the mechanisms whereby AF is *maintained* in the continuous presence of stretch and ACS depends on the interplay between local FDs and reentrant spiral waves.

Methods

Langendorff-perfused Sheep Heart and Stretch-induced AF model

All animal experiments were carried out according to National Institutes of Health guidelines. Twenty-four young sheep (25-30 kg) were anesthetized with sodium pentobarbital (35 mg/kg, IP) then heparinized (200U/kg, IP) with warm oxygenated Tyrode's solution (pH 7.4; 95% O₂, 5% CO₂, 36 to 38 °C). We implemented a model of isolated sheep heart enabling to modify intra-atrial pressure as described previously.^{3,9} After perforation of the intra-atrial septum, we sealed all venous orifices except the inferior vena cava which was connected to a cannula controlling the level of intra-atrial pressure. Intra-atrial pressure was raised to 12 cm H₂O and AF was induced by burst pacing at a cycle length of 10 Hz (10 seconds, 5-ms pulse duration, twice threshold). As previously reported,³ sustained AF episodes (>1 hour) were inducible in all experiments.

Optical Mapping Technique

This technique has been detailed elsewhere,¹⁰ and is presented in the online supplement.

Experimental Protocols

The effects of ACS on SRAF dynamics were examined in detail using various pharmacological protocols in 4 experimental groups (see Table I). Specifically, in groups 1 and 2 ACS was mimicked by simultaneous perfusion of acetylcholine 1 μ M plus isoproterenol 0.03 μ M. To abolish intracellular calcium overload-related triggered activity, we administered ryanodine (RYA) at a concentration of 10-40 μ M¹¹ (Group 1, n=7) or caffeine (CA) 5 mM¹² (Group 2, n=4). In Groups 3 and 4, we assessed the individual effect of RYA or CA respectively, without mimicked ACS. In all groups, optical mapping movies were obtained every 5 minutes after induction of SRAF (see above) and at 15 minutes of AF stabilization. Only those movies obtained between 15 and 30 minutes after drug perfusion were considered for analysis.

Activation Patterns and Dynamics

AF wave patterns were classified into 3 types: (1) rotor, defined as the organizing center of a spiral wave lasting more than one rotation; (2) breakthrough, defined as a wave appearing at the left atrial appendage (LAA) and propagating centrifugally toward the periphery of the field of view; and (3) spatio-temporally organized periodic waves, defined as a minimum of 4 sequential spatio-temporally organized and periodic waves emerging from one edge of the field of view, with similar direction and inter-wave interval.¹⁰ In groups 1 and 2, a representative 1 second movie sample for each animal was analyzed to quantify the number and lifespan of individual rotors, the percentage of time with a visible rotor and the number of breakthroughs.

Numerical Simulations

Numerical simulations were carried out using a 2-dimensional (2D) model to examine how simulated focal discharges impinge on rotor core meandering dynamics. The description of the computer model and of the numerical protocol employed can be found in the online supplement.

Statistical Analysis

Group data were expressed as mean \pm SEM. Frequency data (Figure 1) were compared with a repeated measures, two-way analysis of variance test: 3 (condition; SRAF, ACS and ACS +RYA) \times 3 (location; left atrial roof, left and right atrial appendage). Statistical comparisons of AF dynamics: i) number of breakthroughs ii) number of rotors iii) number of rotations/rotor iv) percentage of time with visible rotor was also performed by two-way ANOVA with Tukey's test. Differences were considered significant when $p < 0.05$.

Results

AF termination

In Table I, we present the overall summary of our 4 experimental groups. In all experiments we obtained sustained episodes of SRAF. ACS was mimicked by the simultaneous perfusion of acetylcholine (1 μ M) and isoproterenol (0.03 μ M). During ACS, only 1/11 SRAF episodes terminated in the presence of RYA (group 1) or CA (group 2). In sharp contrast, 77% (10/13) of SRAF without ACS terminated during perfusion with either RYA 10-40 μ M (group 3) or CA 5 mM (group 4).

Dominant frequencies (DFs) distribution

Figure 1 presents the optical and electrical data on DFs distribution at the LAA and other atrial regions during SRAF, after ACS and ACS+RYA (Group 1). Figure 1A shows a representative DF map (left panel) with corresponding single-pixel recordings (left and

middle tracings) and bipolar electrograms (rightmost tracing) during SRAF in the absence of drugs. The activation frequency at the left atrial (LA) roof (point *a*; orange) was higher than the LAA (point *b*; yellow) and the right atrial appendage (RAA). During ACS (Figure 1B), AF frequency increased at all sites, but in this case DF at the LAA was higher than the LA roof and the RAA. Also, in the setting of ACS+RYA (Figure 1C), the LAA DF tended to be larger than at the LA roof and RAA. The highest frequency corresponded to the red domain, where the LAA single-pixel recording at point *f* exhibited high periodicity and monomorphic morphology (Figure 1C, middle panel).

Panel D summarizes the comparative DF data in all experiments. During SRAF the frequency of activation at the LA roof (7.6 ± 0.7 Hz; white) was significantly higher ($p < 0.05$) than both LAA (6.0 ± 0.3 Hz; black) and RAA (4.3 ± 0.5 Hz; gray). During ACS, DFs significantly increased at all locations compared with SRAF (15.5 ± 0.9 versus 7.6 ± 0.7 Hz at LA roof; 15.7 ± 1.4 versus 6.0 ± 0.3 Hz at LAA; 14.7 ± 2.1 versus 4.3 ± 0.5 Hz at RAA; *, $p < 0.05$). In the presence of ACS, RYA caused significant decreases in DF at both LA roof and RAA without significantly affecting the LAA (10.5 ± 1.5 versus 15.5 ± 0.9 Hz at LA roof; 7.7 ± 1.3 versus 14.7 ± 2.1 Hz at RAA, *, $p < 0.05$; 13.7 ± 1.3 versus 15.7 ± 1.4 Hz at LAA, $p = \text{N.S.}$).

Activation patterns during SRAF

As described previously,³ AF wave propagation during SRAF may be manifest as impulses that are highly periodic both spatially and temporally. As expected, we also observed spatiotemporally periodic waves during SRAF (data not shown). Altogether in 5 animals, AF activation patterns during SRAF were driven by spatiotemporally periodic waves or breakthroughs emerging at varying locations within the LAA; short-lived reentrant wavefronts (1 or 2 rotations) represented $16.6 \pm 5.0\%$ of all the waves analyzed ($n=5$).

ACS associated breakthroughs induce wavebreak, rotor drifting and termination

Figure 2 is a representative example of the 2 types of AF dynamics observed in the presence of ACS. Under these conditions we observed many breakthroughs throughout the LAA which profoundly affected rotor dynamics and lifespan depending on their mutual spatio-temporal relations. In fact, the increased occurrence of breakthroughs during ACS strongly affected the SRAF dynamics in complex ways. First, as shown in Figure 2A, breakthroughs occurring in partially refractory tissue resulted in wavebreak and rotor formation. In this example, at 4188 ms the breakthrough that emerged on the upper LAA underwent wavebreak leading to the formation of a counter-clockwise rotor whose cycle length (72 ms) was equal to the inverse of the maximum DF ($1/DF_{\text{max}}$) in this episode. Second, while several rotors could be observed during a given AF episode, most were forced to drift and eventually terminate after 3 to 4 rotations by their interaction with the repetitively emerging breakthroughs. In Figure 2B and supplemental movie, the breakthrough that appeared near the center of the optical field at frame 956 ms (location 1) forced the nearby rotor 1 to drift over a long distance toward the LA roof (location 2). Collision of the rotor with a second rotor (2) at that location led to its annihilation (see also supplement movie 1).

Breakthroughs force rotors to drift: experimental and numerical study

During ACS, rotors underwent substantial drift. To evaluate rigorously the cause of the drift, we followed the trajectory of the phase singularity (PS) at the rotor tip and quantified the spatio-temporal relationship between PS and breakthrough site as follows: first, as depicted on the left of Figure 2C, the PS-to-center of breakthrough distance at the onset of the breakthrough was noted as *distance a*; i.e., from the asterisk to the white circle in the top frame of Figure 2C. Distance *a* was then plotted against the PS-to-center of breakthrough distance after the rotor had undergone a half rotation; the latter was noted as distance *b* and

measured between the white circles in the top and bottom frames of Figure 2C. As plotted in the rightmost panel (n=4), there was a nonlinear inverse relationship between rotor drifting and PS-breakthrough distance. Breakthroughs caused the most drifting when they occurred in the immediate vicinity of the PS, and the drifting effect tended to fade as the PS-breakthrough distance increased above 0.6 cm.

To provide additional quantitative insight into the cause of drift during ACS, we conducted 2D simulations as depicted in Figure 3. On the left side of panel A, a stationary rotor was established in the 2D sheet and external focal stimuli were applied at 3 different locations from the rotor tip to simulate breakthroughs occurring at varying distances from the rotor's PS as seen in the experiments. As shown on the right side of panel A and in Panel B, the shift in the location of the rotor inversely correlated with the distance between the stimulus and the rotor tip.

AF dynamics changes after abolition of triggered activity

Figure 4A and supplement movie 2 show a representative example of phase movie and the corresponding rotor PS trajectory in the setting of ACS in the presence of RYA (group 1). A long-lasting and stable rotor with a stationary PS trajectory was visualized (Figure 4A upper panels). Notably, a decrease in the number of breakthroughs was also noted. This reentry exhibited the fastest atrial frequency of activation (12.2 Hz). In all animals in Group 1, the rotors were consistently located at the LAA. Similar long-lasting rotors were also observed in all animals during ACS and CA perfusion (Group 2). Figure 4B and supplement movie 3 depict a representative example of a stable dominant rotor located at the anterior LAA and of its corresponding phase and DF maps in the presence of CA.

Figures 5 and 6 summarize the changes in AF dynamics observed in ACS and ACS+RYA or CA. In Figure 5A, ACS increased significantly the number of breakthroughs from 18.8 ± 2.4 /sec in control SRAF to 39.6 ± 4.8 /sec under ACS; in the presence of ACS, RYA significantly decreased the number of breakthroughs to 12.2 ± 2.8 /sec. Furthermore, the number of rotors/sec was dramatically increased under conditions of ACS (Figure 5B). Also the number of rotations/rotor (Figure 6A) was significantly increased from 1.1 ± 0.1 /sec/field-of-view and 1.7 ± 0.3 /sec/field-of-view during SRAF to 2.5 ± 0.4 /sec/field-of-view and 3.0 ± 0.8 /sec/field-of-view after ACS, respectively. Importantly, the number of rotations/rotor after RYA perfusion increased significantly to 6.2 ± 0.9 /sec/field-of-view. Also the percentage of the movie-time with a visible rotor (Figure 6B) progressively increased after ACS and ACS+RYA ($61.4 \pm 10.7\%$ and $93.2 \pm 4.3\%$, respectively vs. $16.6 \pm 5.0\%$ during SRAF). Similar changes in AF dynamics were observed when caffeine was used instead of ryanodine (Figure 5 and 6 right panels).

Discussion

Major Findings

We have employed an experimental model, optical mapping and a pharmacologic approach to investigate the mechanisms of stretch-related AF in the absence and the presence of combined adrenergic and cholinergic input. Our most important results are as follows: 1. In the absence of ACS, the most frequent activation pattern during SRAF was multiple focal discharges manifested as centrifugal breakthroughs. Perfusion of either RYA or CA to abolish calcium release from the SR, and thus prevent focal discharges, resulted in SRAF termination. However perfusion of the same drugs in the presence of ACS did not terminate SRAF. 2. In the presence of ACS, the most common activation pattern during SRAF consisted of multiple short-lived rotors destabilized by a large number of centrifugal breakthrough wavefronts. Breakthroughs consistently impinged on rotor dynamics by

increasing the rate of wavebreak and rotor formation and the amount of rotor drift leading to termination. 3. In sharp contrast, stable and long-lasting reentrant patterns were consistently observed in all ACS experiments after FDs were abolished by RYA or CA.

Mechanism of AF maintenance in the presence of stretch

Our results demonstrate that out of 13 AF episodes associated with atrial stretch in the absence of autonomic input, 10 terminated upon perfusion of RYA or CA. This strongly suggests that in the presence of stretch alone, AF is maintained by spontaneous FDs. Previously we showed that intra-atrial pressures greater than 10 cm H₂O increased the AF frequency. The highest frequencies and greatest spatio-temporal organization were found at the junction between the left superior PV and the left atrium.³ In some cases, short-lived rotors were observed.³ However, at the time we were unable to adequately map optically the PV-posterior left atrial junction of the sheep heart due to the presence of a high density of epicardial fat in that region. This prevented us from being able to definitely establish whether SRAF was maintained by stable rotors or focal discharges or both. The fact that 10/13 SRAF episodes were terminated by RYA or CA perfusion in this new study is, however, indicative that during stretch the arrhythmia is the result of focal discharges emerging from the PV-posterior left atrial junction. Our findings are indeed consistent with studies in the atria of rabbits and monkeys that demonstrated increased rates of spontaneous activity upon mechanical stretch.^{13,14} In turn, the waves generated by such focal discharges have a high propensity for wavebreak early after their onset because of the highly heterogeneous architecture of the posterior wall region. It should be noted, however, that SRAF was maintained in 3 animals despite RYA perfusion suggesting that in some animals both breakthroughs and short-lived reentrant activities were maintaining the fibrillatory activity.

Mechanisms of AF maintenance in the presence of ACS

Multiple studies have investigated the role of the autonomic nervous system in AF generation and maintenance.^{4,6,15} Some such studies⁵ have focused on the manner in which cholinergically mediated APD shortening secondary to K_{ACh} channel activation, together with adrenergically induced increase in intracellular calcium release from the sarcoplasmic reticulum, leads to DADs and/or late phase-3 EADs, through a mechanism which most likely involves an increase in the forward mode activity of the sodium-calcium exchanger.¹¹ However, until now, the mechanisms of AF maintenance in the presence of combined ACS remained poorly explored. The above publications suggested that focal discharges may be sufficient to maintain AF but previous work strongly argued in favour of the idea that vagally-induced reentrant sources in the left atrium maintain the fibrillatory activity.¹⁵⁻¹⁷

To the best of our knowledge, this is the first attempt to examine the mechanisms of AF maintenance in the presence of stretch and ACS and to evaluate the respective roles of focal discharges and reentry in those mechanisms. We demonstrate that in the absence of autonomic input, focal discharges emerging from the PV-posterior left atrial junction prevail as the mechanism that maintains SRAF. On the other hand, in the presence of ACS, SRAF is maintained by the dynamic interaction between waves generated by stretch-induced, adrenergically enhanced focal discharges and waves that emanate repeatedly from relatively unstable rotors. Hence, we propose that FDs play a dual role in AF dynamics: they enhance the likelihood of wavebreak and new rotor formation but at the same time they destabilize existing rotors forcing them to drift and eventually terminate.

Mechanism of increased of rotor destabilization by FDs

Our experiments and numerical simulations establish a strong relationship between the FDs emerging as breakthroughs in the vicinity of a rotor and the increased propensity of the rotor

to drift. The data provide a solid explanation as to how two apparently mutually exclusive mechanisms, reentry and focal activity interact to maintain SRAF in the presence of ACS. It should be mentioned, however, that the paradigm of rotors destabilization by paced waves has been presented in previous works. For instance, Gottwald et al, suggested that rotors could be forced to drift by the application of external stimuli of the appropriate characteristics.¹⁸ Subsequently, Davidenko et al. experimentally demonstrated that externally induced waves may collide with a self-sustaining spiral and result in rotor annihilation, multiplication or in a shift of the spiral core.¹⁹ As shown in Figure 2 and 3, our results bring such phenomena into the context of AF for the first time. They provide both qualitative and quantitative demonstration that the increased number of FDs observed during ACS contributes to reentrant SRAF maintenance by inducing substantial rotor drifts, and leading to either wavebreak formation or rotor termination, or both. Notably, experiments and numerical simulations show strikingly similar results that emphasize how determinant the location of the focal discharge is for rotor drift. As also suggested recently by the studies of Huffaker et al.²⁰ and Agladze et al.²¹ FDs that appear in the vicinity of the rotor core cause large drifts and may lead to spiral termination, while FDs occurring at large distances from the core had virtually no effect on the rotor dynamics (see Figures 2B and 3). In our experiments, 0.6 cm was found to be an approximate limit above which virtually no rotor drift was observed. Furthermore, the data on AF termination presented in Table 1 suggest that both FDs and reentrant mechanisms co-exist and interplay to maintain AF in the presence of ACS. Indeed, virtually none of the ACS-maintained AF episodes terminated after FDs were abolished.

Mechanism of FDs

While the breakthroughs observed as centrifugal AF waves could be caused by either a reentrant or a focal discharge mechanism, our experimental results are strongly indicative of an afterdepolarization-induced focal discharge mechanism. In the online supplement figure 1, the post-pacing interval of spontaneous centrifugal breakthroughs after a 5-second rapid pacing burst at various cycle lengths was measured. As shown in panel A of that figure, the post-pacing interval correlated with the basic cycle length of stimulation, which is strongly suggestive of an after-depolarization mechanism while a negative correlation would have been expected for a reentrant mechanism. These results, together with the sharp decrease in the incidence of breakthroughs upon RYA or CA perfusion (Figure 5), are indicative of a causal link between afterdepolarization induced focal discharges and the breakthrough waves patterns visualized during AF initiation and maintenance.

Limitations

The pharmacological approach to abolish FDs could have been optimized by the perfusion of thapsigargin and ryanodine as described by Chou et al.²² Besides, neurally-mediated ACS is a rather complex phenomenon involving the interaction of the exogenous autonomic nervous system modulated by neural activity at atrial ganglionated plexi.²³ Thus the present findings will need to be extended to whole animal models with intact autonomic cardiac innervation. In addition, a thorough evaluation of AF termination mechanisms would have to include AF dynamics analysis at the time of termination. Finally, various types of paced wave-spiral wave interactions such as direct spiral annihilation or spiral multiplication have been previously described¹⁹ and are likely to have also been played a role in AF dynamics in the presence of ACS.

Conclusions

We demonstrate that abolishing FDs was not sufficient to terminate AF in the presence of ACS. However, FD suppression dramatically changed ACS-related AF dynamics and terminated SRAF in the absence of ACS. In the clinical realm, radiofrequency delivery in

the area of the left atrium containing ganglionated plexi is the basis of some of the AF ablation strategies currently used in AF patients.⁷ It is commonly considered that localized left atrial ganglionated plexi have the propensity to elicit local FDs and to initiate or maintain AF. However, the mechanisms of AF maintenance and the exact mechanistic benefit of abolishing ganglionated plexi discharges by RF are unknown. Potentially, our findings could provide the basis for future investigations on the failure of some cases of AF ablation strategies that specifically target AF triggers elimination.

Supplementary Material

Refer to Web version on PubMed Central for supplementary material.

Acknowledgments

We thank Jianling Deng and Jiang Jiang for their technical assistance.

This work was supported in part by National Heart Lung and Blood Institute grants PO1 HL039707, PO1 HL087226 and RO1 HL070074 to JJ; RO1-HL087055 and ACCF/GE Healthcare Career Development Award to JK; Heart Rhythm Society Fellowship Award 2007-8, the Suzuken Memorial Foundation 2006-7, the Kowa Life Science Foundation 2006 to MY; and a grant from the Centro Nacional de Investigaciones Cardiovasculares (CNIC) of Spain (JJ).

Abbreviations

ACS	adreno-cholinergic stimulation
AF	atrial fibrillation
APD	action potential duration
CA	caffeine
DAD	delayed after-depolarizations
DF	dominant frequency
EAD	early after-depolarizations
FD	focal discharge
K, ACh	acetylcholine activated potassium
LAA	left atrial appendage
LA roof	left atrial roof
PS	phase singularity
RAA	right atrial appendage
RYA	ryanodine
SACs	stretch activated channels
SRAF	stretch-related AF
2D	2-dimensional

References

1. Vaziri SM, Larson MG, Benjamin EJ, et al. Echocardiographic predictors of nonrheumatic atrial fibrillation. The Framingham Heart Study. *Circulation* 1994;89:724–730. [PubMed: 8313561]

2. Manyari DE, Patterson C, Johnson D, et al. Atrial and ventricular arrhythmias in asymptomatic active elderly subjects: correlation with left atrial size and left ventricular mass. *Am Heart J* 1990;119:1069–1076. [PubMed: 2330865]
3. Kalifa J, Jalife J, Zaitsev AV, et al. Intra-atrial pressure increases rate and organization of waves emanating from the superior pulmonary veins during atrial fibrillation. *Circulation* 2003;108:668–671. [PubMed: 12900337]
4. Coumel P. Cardiac arrhythmias and the autonomic nervous system. *J Cardiovasc Electrophysiol* 1993;4:338–355. [PubMed: 8269304]
5. Patterson E, Po SS, Scherlag BJ, et al. Triggered firing in pulmonary veins initiated by in vitro autonomic nerve stimulation. *Heart Rhythm* 2005;2:624–631. [PubMed: 15922271]
6. Elvan A, Pride HP, Eble JN, et al. Radiofrequency catheter ablation of the atria reduces inducibility and duration of atrial fibrillation in dogs. *Circulation* 1995;91:2235–2244. [PubMed: 7697854]
7. Schauerte P, Scherlag BJ, Pitha J, et al. Catheter ablation of cardiac autonomic nerves for prevention of vagal atrial fibrillation. *Circulation* 2000;102:2774–2780. [PubMed: 11094046]
8. Burashnikov A, Antzelevitch C. Late-phase 3 EAD. A unique mechanism contributing to initiation of atrial fibrillation. *Pacing Clin Electrophysiol* 2006;29:290–295. [PubMed: 16606397]
9. Ravelli F, Allesie M. Effects of atrial dilatation on refractory period and vulnerability to atrial fibrillation in the isolated Langendorff-perfused rabbit heart. *Circulation* 1997;96:1686–1695. [PubMed: 9315565]
10. Skanes AC, Mandapati R, Berenfeld O, et al. Spatiotemporal periodicity during atrial fibrillation in the isolated sheep heart. *Circulation* 1998;98:1236–1248. [PubMed: 9743516]
11. Patterson E, Lazzara R, Szabo B, et al. Sodium-calcium exchange initiated by the Ca²⁺ transient: an arrhythmia trigger within pulmonary veins. *J Am Coll Cardiol* 2006;47:1196–1206. [PubMed: 16545652]
12. Aronson RS, Cranefield PF, Wit AL. The effects of caffeine and ryanodine on the electrical activity of the canine coronary sinus. *J Physiol* 1985;368:593–610. [PubMed: 4078750]
13. Chang SL, Chen YC, Chen YJ, et al. Mechanoelectrical feedback regulates the arrhythmogenic activity of pulmonary veins. *Heart* 2007;93:82–88. [PubMed: 16905626]
14. Kaufmann R, Theophile U. Autonomously promoted extension effect in Purkinje fibers, papillary muscles and trabeculae carneae of rhesus monkeys. *Pflugers Arch Gesamte Physiol Menschen Tiere* 1967;297:174–189.
15. Sarmast F, Koli A, Zaitsev A, et al. Cholinergic atrial fibrillation: I(K,ACh) gradients determine unequal left/right atrial frequencies and rotor dynamics. *Cardiovasc Res* 2003;59:863–873. [PubMed: 14553826]
16. Mandapati R, Skanes A, Chen J, et al. Stable microreentrant sources as a mechanism of atrial fibrillation in the isolated sheep heart. *Circulation* 2000;101:194–199. [PubMed: 10637208]
17. Atriaenza F, Almendral J, Moreno J, et al. Activation of inward rectifier potassium channels accelerates atrial fibrillation in humans: evidence for a reentrant mechanism. *Circulation* 2006;114:2434–2442. [PubMed: 17101853]
18. Gottwald G, Pumir A, Krinsky V. Spiral wave drift induced by stimulating wave trains. *Chaos* 2001;11:487–494. [PubMed: 12779486]
19. Davidenko JM, Salomonsz R, Pertsov AM, et al. Effects of pacing on stationary reentrant activity. Theoretical and experimental study. *Circ Res* 1995;77:1166–1179. [PubMed: 7586230]
20. Huffaker RB, Weiss JN, Kogan B. Effects of early afterdepolarizations on reentry in cardiac tissue: a simulation study. *Am J Physiol Heart Circ Physiol* 2007;292:H3089–3102. [PubMed: 17307992]
21. Agladze K, Kay MW, Krinsky V, et al. Interaction between spiral and paced waves in cardiac tissue. *Am J Physiol Heart Circ Physiol* 2007;293:H503–513. [PubMed: 17384124]
22. Chou CC, Nguyen BL, Tan AY, et al. Intracellular calcium dynamics and acetylcholine-induced triggered activity in the pulmonary veins of dogs with pacing-induced heart failure. *Heart Rhythm* 2008;5:1170–1177. [PubMed: 18554987]
23. Chen PS, Douglas P. Zipes Lecture. Neural mechanisms of atrial fibrillation. *Heart Rhythm* 2006;3:1373–1377. [PubMed: 17074648]

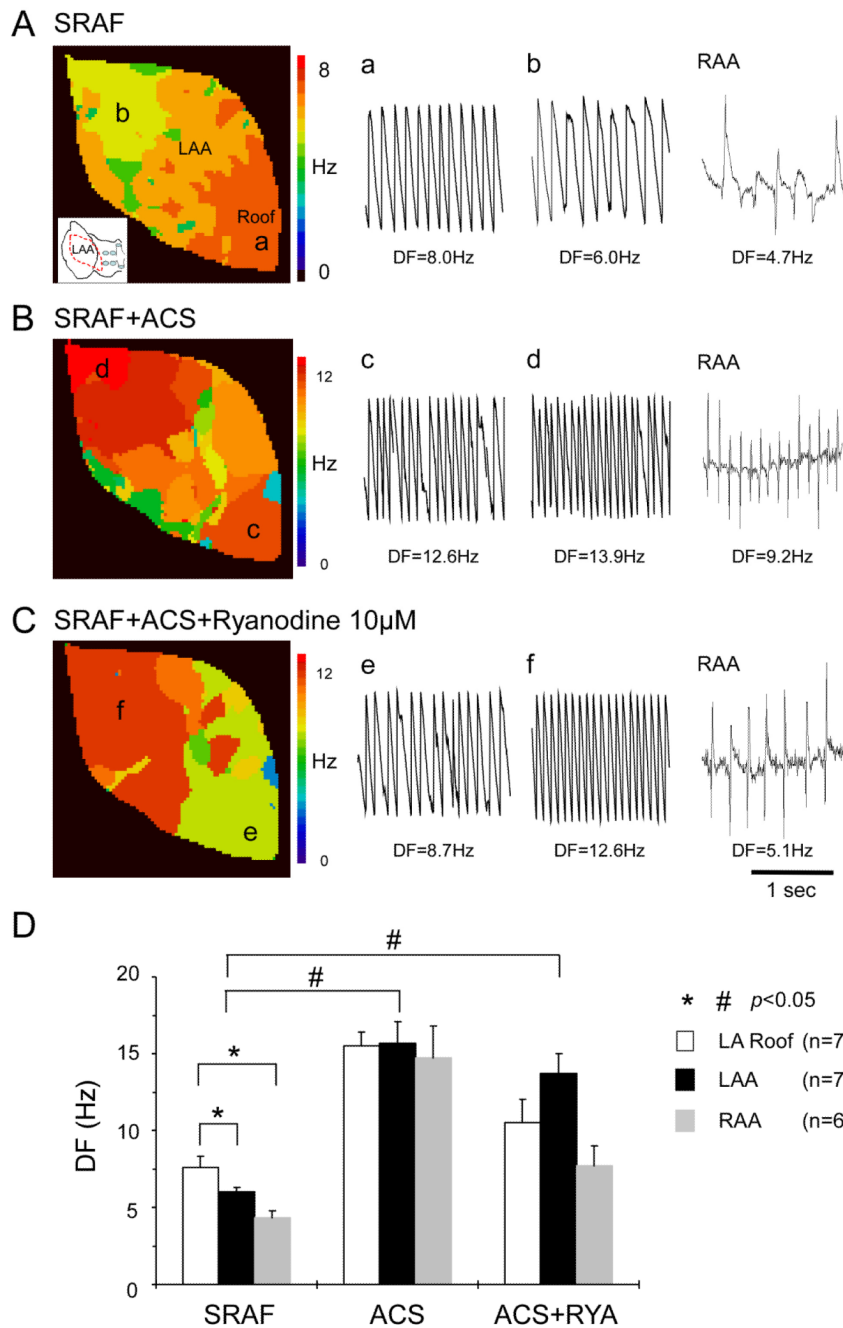


Figure 1. DFs changes during SRAF in the presence of ACS and RYA. **A-C**, Representative LAA DF maps together with single-pixel recordings at locations **a-f** as well as corresponding RAA electrograms during: **A**: SRAF **B**: ACS **C**: ACS+RYA. **D**, DFs at the LA roof, LAA and RAA during SRAF, ACS and ACS+RYA. LA roof DFmax during SRAF was significantly higher than DFs at both LAA and RAA (* and #: $p<0.05$).

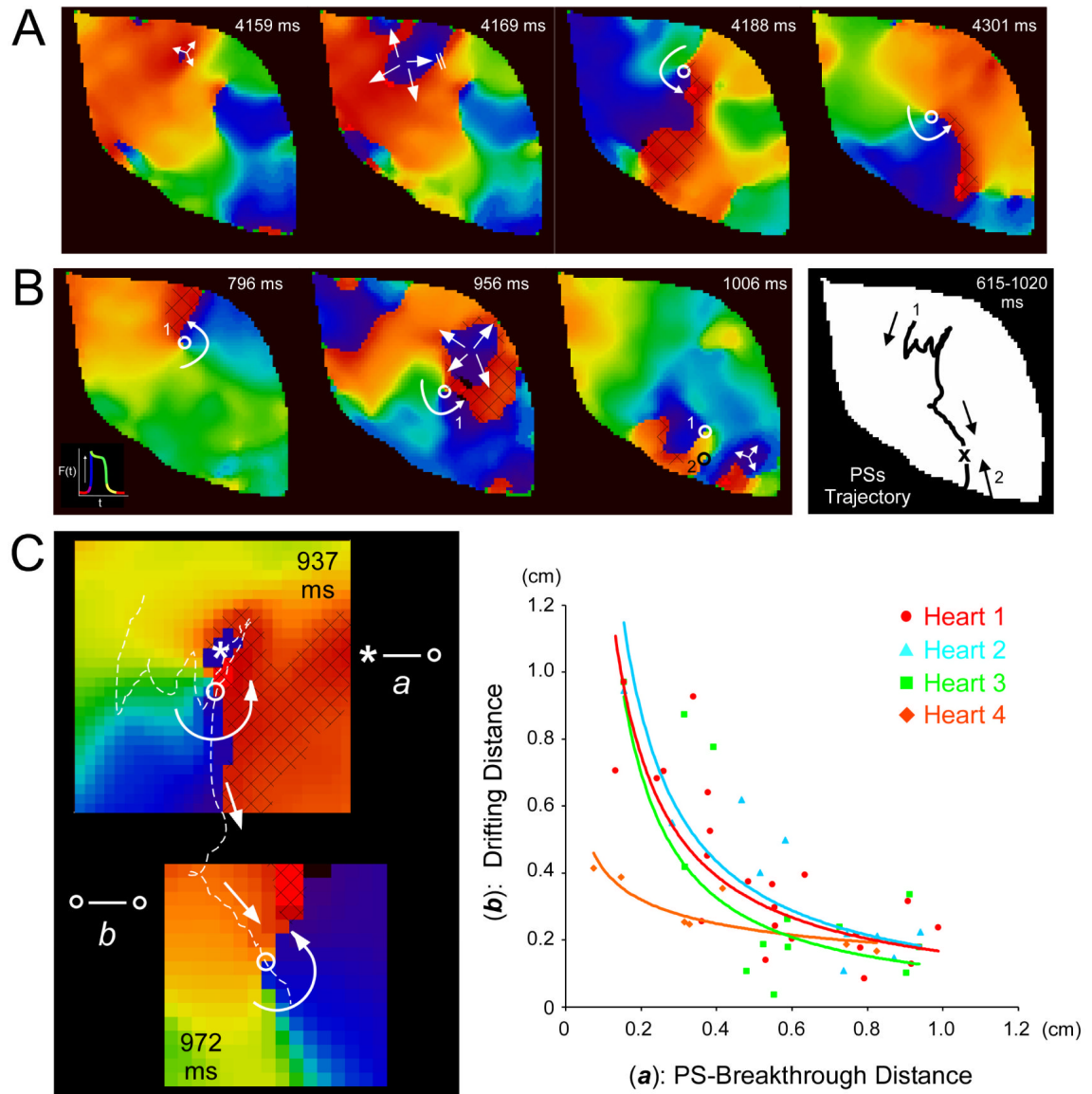


Figure 2.

Interaction between rotors and spontaneous breakthroughs in the setting of ACS. **A**, Representative phase maps during ACS; repeated breakthroughs gave rise to rotor formation after wavebreak. **B**, *Left*, a breakthrough induced substantial rotor drift. *Right*, the corresponding PS trajectory is shown for rotor 1, which was forced to drift inferiorly and terminate after collision with counter-rotating rotor 2; both rotors mutually annihilated. **C**, Quantification of breakthrough-induced-rotor drift. *Left*, example of measurements between PS and breakthrough center (distance **a**: asterisk to open circle) and breakthrough induced-rotor drifting (distance **b**: between open circles) in the presence of ACS. *Right*, relationship between (**a**) and (**b**) (heart 1: same experiment as in Figure 1). We added a trendline to fit a line according to a power function $y=x^n$. A black shaded area depicts the excitable gap for the rotors presented.

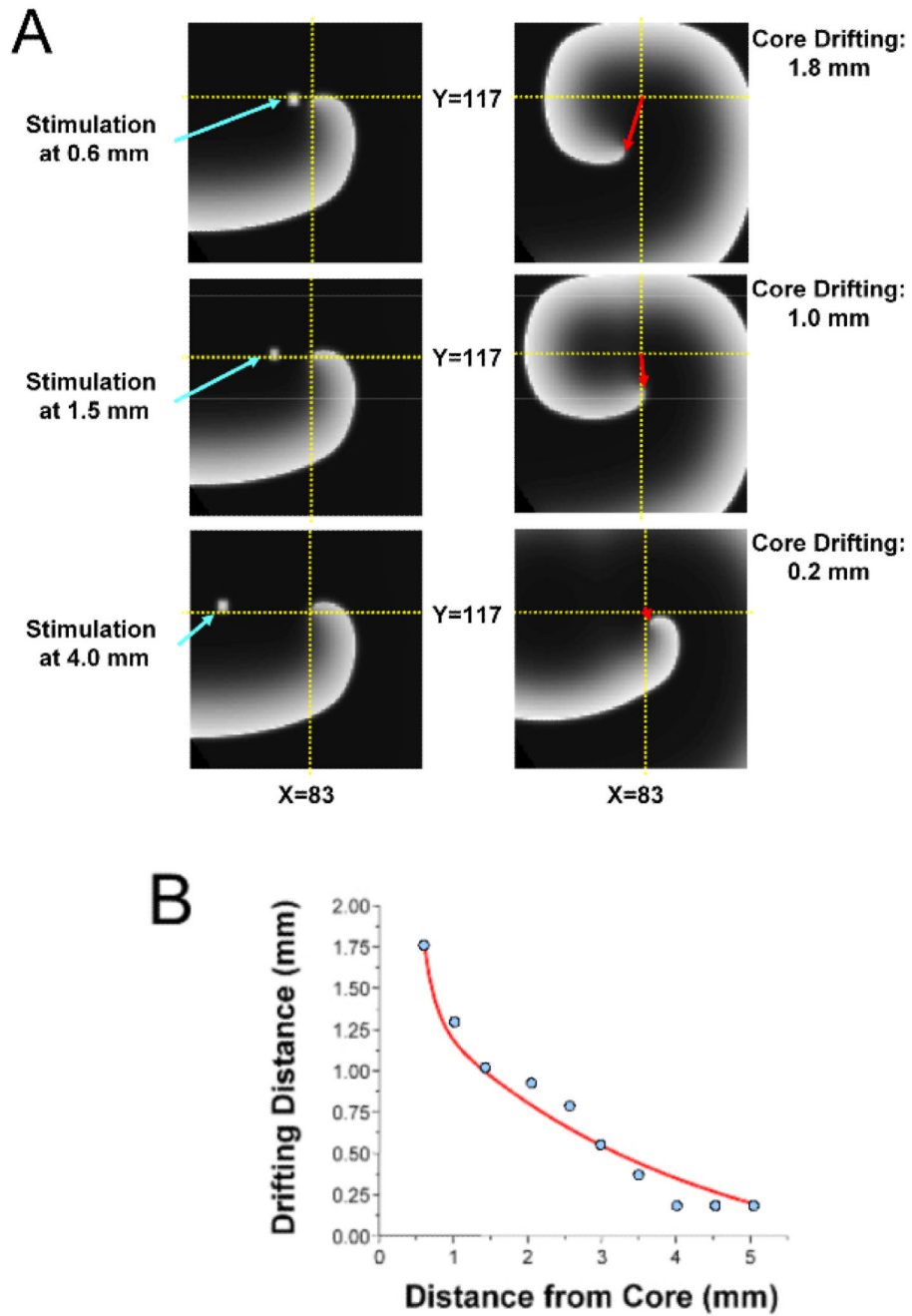


Figure 3. Numerical simulation: Focal stimulus induces rotor shift. A, Snapshots of reentrant activity showing distance between stimulus location and core center (*left*), and amount of induced core shift (*right*). B, Plot of shift as a function of stimulus distance from rotor center shows inverse relation similar to that demonstrated in the experiment (Figure 2).

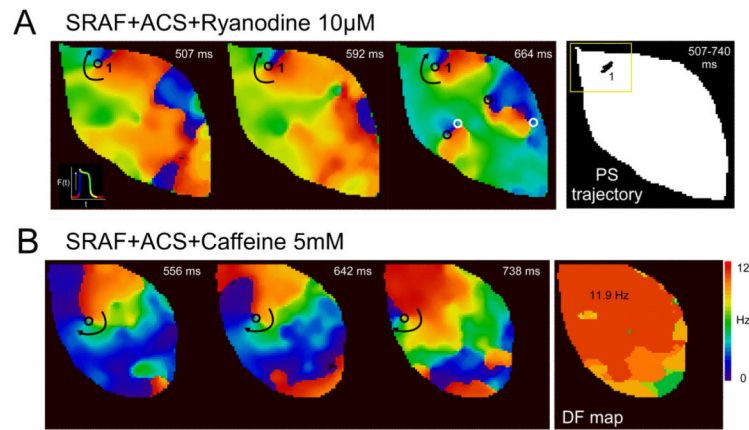


Figure 4. Long-lasting rotors in the setting of SRAF during ACS+RYA 10 μ M (A) or ACS+CA, 5 mM (B). **A**, *Upper left panel*, long-lasting rotor (*left*) with a very stationary PS trajectory (*right*) that showed minimal meandering. **B**, Three snapshots of a representative phase movie and of the corresponding DF map during an SRAF episode in the presence of ACS+CA are shown. PSs are indicated by circles (black for clockwise rotation, white for counter-clockwise rotation).

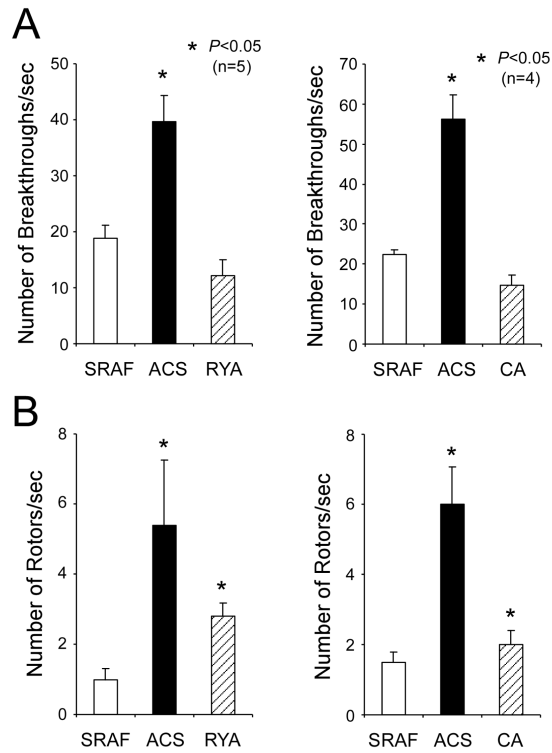


Figure 5. Effects of ACS, ACS+RYA (Group 1) and ACS+CA (Group 2) on the number of breakthrough (**A**) and rotors/sec (**B**) during stretch-related AF. (*: $p < 0.05$ vs SRAF.)

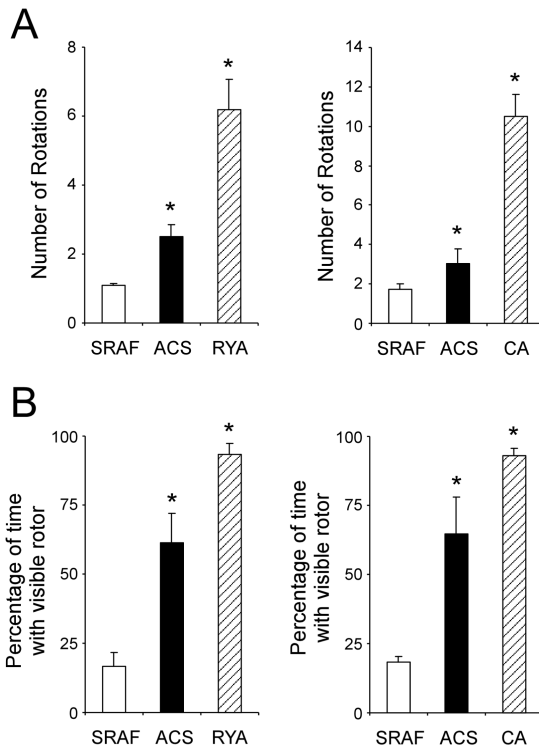


Figure 6. Effects of ACS, ACS+RYA (Group 1) and ACS+CA (Group 2) on the number of rotations (A) and percentage of time with visible rotor (B) during stretch-related AF. (*: $p < 0.05$ vs SRAF.)

Table 1

Experimental Protocols and AF Termination

	Drug 1		Drug 2	Termination
Group 1	SARF →	ACS Isoproterenol 0.03µM +Acetylcholine 1µM	Ryanodine 10-40µM	→ 1/7
Group 2	SRAF →	ACS Isoproterenol 0.03µM +Acetylcholine 1µM	Caffeine 5mM	→ 0/4
Group 3	SRAF →		Raynodine 10-40µM	→ 6/9
Group 4	SRAF →		Caffeine 5mM	→ 4/4